

Hydrocarbon anions in interstellar clouds and circumstellar envelopes

T. J. Millar, C. Walsh and M. A. Cordiner

Astrophysics Research Centre, School of Mathematics and Physics, Queen's University Belfast, Belfast BT7 1NN, Northern Ireland

`Tom.Millar@qub.ac.uk, cwalsh13@qub.ac.uk, m.cordiner@qub.ac.uk`

and

R. Ní Chuimín

Jodrell Bank Centre for Astrophysics, School of Physics and Astronomy, University of Manchester, Sackville St., Manchester M60 1QD, UK

`Roisin.Ni-Chuimin@manchester.ac.uk`

and

Eric Herbst

Departments of Physics, Chemistry and Astronomy, The Ohio State University, Columbus, OH 43210-1106

`herbst@mps.ohio-state.edu`

ABSTRACT

The recent detection of the hydrocarbon anion C_6H^- in the interstellar medium has led us to investigate the synthesis of hydrocarbon anions in a variety of interstellar and circumstellar environments. We find that the anion/neutral abundance ratio can be quite large, on the order of at least a few percent, once the neutral has more than five carbon atoms. Detailed modeling shows that the column densities of C_6H^- observed in IRC+10216 and TMC-1 can be reproduced. Our calculations also predict that other hydrocarbon anions, such as C_4H^- and C_8H^- , are viable candidates for detection in IRC+10216, TMC-1 and photon-dominated regions such as the Horsehead Nebula.

Subject headings: astrochemistry — ISM: abundances — ISM: molecules — ISM: clouds — stars: carbon

1. Introduction

The recent detection of C_6H^- in the carbon-rich AGB star IRC+10216 and the cold, dense interstellar cloud TMC-1 by McCarthy et al. (2006) with abundance ratios relative to C_6H of 0.01–0.1 indicates that anions may play a more significant role in interstellar physics and chemistry than heretofore believed.

The possibility that a relatively large fraction of molecular material in interstellar clouds might be in the form of anions was first suggested by Herbst (1981) who pointed out that carbon chain molecules and other radicals have large electron affinities, leading to high radiative attachment rates such as those measured by Woodin et al. (1980) with the attendant possibility of anion/neutral fractions on the order of a few percent. More recently, it has been recognized that PAH anions could soak up a significant fraction of the free electrons in interstellar clouds and alter the charge balance to a significant degree (Lepp & Dalgarno 1988a) as well as providing significant heating through photodetachment of electrons in diffuse clouds (Lepp & Dalgarno 1988b). Petrie (1996) has investigated the synthesis of CN^- by the dissociative attachment of $MgCN$ and $MgNC$ and other mechanisms, while Petrie & Herbst (1997) showed that C_3N^- could be detectable in interstellar clouds. The study of large hydrocarbons anions received some attention following the observation by Tulej et al. (1998) that absorption bands in several carbon-chain anions coincided with several of the diffuse interstellar bands. Subsequently, the formation of such species in diffuse clouds was studied by Ruffle et al. (1999) who showed, in particular, that C_7^- was unlikely to be a source for any DIBs. Millar et al. (2000) considered the formation of hydrocarbon anions containing more than six carbon atoms in the carbon-rich circumstellar envelope of IRC+10216 and showed that appreciable column densities could arise in the outer envelope.

2. Chemical Model

The basic route to the formation of anions is electron radiative attachment:



which has been discussed in the context of bare carbon chains by Terzieva & Herbst (2000). The rate coefficients of relevant processes have not been experimentally determined at low temperatures and in this work we have used phase-state theory assuming *s*-wave attachment with radiative stabilisation occurring by vibrational and electronic transitions (Terzieva & Herbst 2000). Table 1 contains some relevant attachment rate coefficients. The calculations of rates for these and other processes will be discussed in a separate paper (Herbst, in preparation). For C_nH radicals, we find that radiative attachment occurs at the

collisional rate once the number of carbon atoms is larger than five; for C_4H , the attachment efficiency is only around 1%. Barckholtz et al. (2001) have shown experimentally that neither carbon-chain anions nor hydrocarbon anions react with H_2 but do so with H atoms. We have also included loss reactions of anions with C , C^+ , C_2H_2^+ (in IRC+10216), and photons, with all cation-anion rate coefficients taken to be $10^{-7} \text{ cm}^3 \text{ s}^{-1}$. For the photodetachment rates, some of which are shown in Table 1, we have assumed the cross section σ to depend on photon energy ϵ via the relation

$$\sigma = \sigma_0(1 - EA/\epsilon)^{0.5}, \epsilon \geq EA, \quad (2)$$

where $\sigma_0 = 1.0 \times 10^{-17} \text{ cm}^2$ and EA is the electron affinity of the neutral molecule. Relevant electron affinities have been obtained from theoretical and experimental results (Herbst, in preparation). The UV radiation field as described by Mathis et al. (1983) has been adopted. We have extended earlier models such as that by Ruffle et al. (1999), which included C_n^- , $n = 7-23$, and by Millar et al. (2000), which included C_nH^- , $n = 7-23$, down to anions containing four carbon atoms following the determination of the microwave spectrum of C_4H^- by Gupta et al. (2007).

In addition to the reactions discussed above, we have included in the CSE and PDR models radiative association between carbon-chain anions and neutrals leading to carbon chains of up to 23 carbon atoms (Millar et al. 2000), while in the dark cloud models we have included reactions between anions and O atoms, with a rate coefficient of $10^{-10} \text{ cm}^3 \text{ s}^{-1}$, unless specifically measured (Eichelberger et al. 2002).

3. Results

3.1. Circumstellar Envelope

We model the carbon-rich AGB star IRC+10216 using the numerical model developed by Millar et al. (2000) and Millar (2003). They modelled the formation of anions with more than six carbon atoms and showed that the anion radial distribution could extend beyond 10^{17} cm and relative to their neutral analogues, abundance ratios approaching 0.1 (for C_7^- , for example) could be achieved. Some results of our present calculation in which we have extended our species down to C_4H^- are shown in Table 2 and Figure 1. Our results show that column densities of $1.0 \times 10^{13} \text{ cm}^{-2}$ for C_4H^- to $2.3 \times 10^{13} \text{ cm}^{-2}$ for C_{10}H^- are achievable, with anion-to-neutral column density ratios of 0.008 for C_4H to around 0.3–0.4 for C_6H , C_8H and C_{10}H . Note that although the electron attachment efficiency for C_4H is only around 1% that of C_6H and C_8H , C_4H^- has a relatively large column density since C_4H is more abundant. Both C_4H^- and C_8H^- are candidates for detection in IRC+10216. In the

region interior to a radial distance of 8×10^{16} cm, the main loss of anions occurs through reaction with H atoms, while mutual neutralisation with C⁺ dominates in $(1.8 - 13) \times 10^{17}$ cm. Elsewhere photodetachment is the major loss route.

McCarthy et al. (2006) measured a C₆H[−] column density of 3×10^{12} cm^{−2}, approximately 60 times less than is produced in our model. Although the column density is over-produced, it is important to note that the column densities of the large hydrocarbon chains are very sensitive to the initial abundance of acetylene adopted in the model. This results from the fact that the most efficient method of growth is via the addition of C₂ units. For example, if the initial abundance of C₂H₂ is reduced by five, the column density of C₆H is reduced by about 45 and that of C₁₀H by 100. The anion column densities are not affected as much, typically reducing by about an order of magnitude, since less acetylene also leads to a reduction in the abundances of H atoms and C⁺ in the envelope. The observed anion-to-neutral ratio is 0.01–0.1 where the range is due to the range of reported C₆H column densities (Kawaguchi et al. 1995; Guélin et al. 1997), but is in reasonable agreement with the calculated value of 0.3, given the uncertainties in the rates of anion formation (by radiative electron attachment), and destruction.

Finally we note that the anion abundances can be greater than that of free electrons in the region around 5×10^{16} cm. This reflects the efficiency of carbon-chain growth and electron attachment. A similar result is found in dark cloud models when PAHs are included (Lepp & Dalgarno 1988a).

3.2. Dark Clouds

Here we adopt parameters applicable to the cold dust cloud TMC-1 ($n(\text{H}_2) = 2 \times 10^4$ cm^{−3}, T = 10 K, A_V = 10 mag.) and perform quasi-time-dependent modeling. The initial elemental abundances of C, N and O relative to H are 7.30×10^{-5} , 2.14×10^{-5} and 1.76×10^{-4} , respectively. Figure 2 shows the time-dependent evolution of the fractional abundances (with respect to H₂) of C₄H[−] and C₆H[−] and their corresponding neutrals from 10⁴ yr while Table 3 and Table 4 present anion column densities and anion/neutral ratios respectively, at both early-time (3.16×10^5 yr) and steady state ($> 10^8$ yr). We adopt N(H₂) = 10²² cm^{−2} in calculating the molecular column densities.

Steady-state abundances are very low due to the incorporation of carbon into CO but much better agreement occurs at earlier times in the evolution. The column density of C₆H[−] produced in our model at early time (3.16×10^5 yr), 1.35×10^{11} cm^{−2}, is very close to that observed by McCarthy et al. (2006), 1×10^{11} cm^{−2}. We calculate the column density of

the neutral C_6H at early time to be $2.58 \times 10^{12} \text{ cm}^{-2}$, which is in good agreement with the observed value of $4.10 \times 10^{12} \text{ cm}^{-2}$ (Bell et al. 1999). The observed anion-to-neutral ratio is 0.025, which is in very good agreement with the calculated early-time value of 0.052, given the uncertainties in assorted rate coefficients.

3.3. Photon-Dominated Regions

We have used the code developed by the Meudon group (Le Petit et al. 2006) with the additional hydrocarbon chemistry described above. For this model we assume a fixed temperature of 50 K and parameters representative of those in the Horsehead Nebula; i.e., $G = 60G_0$, where G_0 is the interstellar UV radiation field, $A_V = 10 \text{ mag}$. to the cloud center, and a total hydrogen density of $2 \times 10^4 \text{ cm}^{-3}$. These models are steady-state, which is achieved rapidly due to the enhanced UV field and fast photodestruction rates. The PDR models show that the anionic species formed can survive exposure to a high radiation field present in regions such as the Horsehead Nebula because, given the high electron abundance, the formation path of electron attachment is efficient enough to overcome the rapid photodetachment of the fragile anions. This high electron abundance at low to intermediate extinction can be inferred from the C^+ abundance in Fig. 3, which also shows that significant abundances of the anions arise at low extinction ($A_V \sim 1.5\text{--}3 \text{ mag}$). At low A_V , $\sim 0.5\text{--}2 \text{ mag}$., the dominant loss of anions is through mutual neutralisation with C^+ (and to a lesser extent through reactions with atomic hydrogen). Thus, since $n(C^+) = n(e)$ in this region, the anion/neutral abundance ratio depends on the ratio of the rate coefficients for electron attachment and mutual neutralisation. For species with more than five carbon atoms, this leads to abundance ratios greater than unity; for smaller species, the ratio is less than one. In fact, the abundances of the anions are, in some cases, larger than the neutral species. Relevant results are listed in Table 5. Most notably, C_8H^- and $C_{10}H^-$ are more dominant than the neutral species with fractional abundances over an order of magnitude greater than those of C_8H and $C_{10}H$.

Since the PDR model provides abundances perpendicular to the line-of-sight for a PDR seen edge on, as is the case for the Horsehead Nebula, it is more appropriate to compare fractional abundances rather than column densities. The peak abundance of C_4H is consistent with observations of the Horsehead region made by Teyssier et al. (2004). Although the relative abundance of C_4H^- (3.5%) to its neutral analog is not as high as C_6H^- or C_8H^- , the higher abundance of the neutral species allows a significantly large absolute value of this anion to be formed. The C_6H^- anion has a peak abundance of 4.7 times that of the neutral species. The detection of C_6H in the Horsehead Nebula was reported by Teyssier et al.

(2004), who calculated a peak abundance relative to H_2 of 1.0×10^{-10} , about one order of magnitude greater than calculated. It is possible that we are missing an important formation mechanism in this environment. One possibility is that hydrocarbon abundances are boosted by destruction of PAH particles, rather than being synthesized from smaller species. In any case, our anion/neutral ratios are independent of the mode of formation of the neutral.

4. Conclusion

We find that electron attachment to hydrocarbon molecules is very efficient for species containing more than five carbon atoms. The anions are created so efficiently that they can be abundant even in regions where they are destroyed rapidly by photons, such as CSEs and PDRs, and in dark clouds, despite the low fractional abundance of electrons. In particular, we find that anions such as C_6H^- , C_8H^- and C_{10}H^- can have abundances relative to their neutral analogs ranging from a few percent to greater than unity, while C_4H^- , although formed relatively inefficiently through electron attachment, can be observable in astronomical objects, given the large column densities of C_4H detected. In fact, as this paper was being prepared, we became aware of a preprint by Cernicharo et al. in which the detection of C_4H^- in IRC+10216 is reported with a $\text{C}_4\text{H}^-/\text{C}_6\text{H}^-$ column density ratio of 1/7, compared to our calculated value of 1/17.

Astrophysics at QUB is supported by a grant from PPARC. RNC and TJM are supported by the European Community's human potential programme under contract MCRTN-CT-512302, 'The Molecular Universe', CW by a scholarship from the Northern Ireland Department of Employment and Learning, and MAC by QUB. EH acknowledges support for his research program in astrochemistry by the National Science Foundation. We thank Dr. Aigen Li for providing us his code to calculate radiation intensity as a function of wavelength and extinction.

REFERENCES

Avery, L. W., Amano, T., Bell, M. B., Feldman, P. A., Johns, J. W. C., MacLeod, J. M., Matthews, H. E., Morton, D. C., Watson, J. K. G., Turner, B. E., Hayashi, S. S., Watt, G. D., & Webster, A. S. 1992 ApJS, 83, 363

Barckholtz, C., Snow, T. P., & Bierbaum, V. M. 2001, ApJ, 547, L171

Bell, M. B., Feldman, P. A., Watson, J. K. G., McCarthy, M. C., Travers, M. J., Gottlieb, C. A., & Thaddeus, P. 1999, *ApJ*, 518, 740

Dayal, A., & Bieging, J. H. 1993, *ApJ*, 407, L37

Eichelberger, B., Barckholtz, C., Stepanovic, M., Bierbaum, V. M., & Snow, T. P. 2002, NASA Laboratory Astrophysics Workshop, ed. F. Salama, NASA/CP-2002-21186, p. 120

Guélin, M., Friberg, P., & Mezaoui, A. 1982, *A&A*, 109, 23

Guélin, M., Cernicharo, J., Travers, M. J., McCarthy, M. C., Gottlieb, C. A., Thaddeus, P., Ohishi, M., Saito, S., & Yamamoto, S. 1997, *A&A*, 317, L1

Gupta, H. C., Brünken, S., Tamassia, F., Gottlieb, C. A., McCarthy, M. C., & Thaddeus, P. 2007, *ApJ*, 655, L57

Herbst, E. 1981, *Nature*, 289, 656

Kawaguchi K., Kasai, Y., Ishikawa, S., & Kaifu, N. 1995, *PASP*, 47, 853

Le Petit, F., Nehmeé, C., Le Bourlot, J., & Roueff, E. 2006, *ApJS*, 164, 506

Lepp, S., & Dalgarno, A. 1988a, *ApJ*, 324, 553

Lepp, S., & Dalgarno, A. 1988b, *ApJ*, 335, 769

Mathis, J. S., Mezger, P. G., & Panagia, N. 1983, *A&A*, 128, 212

McCarthy, M. C., Gottlieb, C. A., Gupta, H. C., & Thaddeus, P. 2006, *ApJ*, 652, L141

Millar, T. J. 2003, in *Asymptotic Giant Branch Stars*, eds. H. J. Habing & H. Olofsson, New York: Springer, 247

Millar, T. J., Herbst, E., & Bettens, R. P. A. 2000, *MNRAS*, 316, 195

Petrie, S. 1996, *MNRAS*, 281, 137

Petrie, S., & Herbst, E. 1997, *ApJ*, 491, 210

Ruffle, D. P., Bettens, R. P. A., Terzieva, R., & Herbst, E. 1999, *ApJ*, 523, 678

Terzieva, R., & Herbst, E. 2000, *Int. J. Mass Spectrom.*, 201, 135

Teyssier, D., Fossé, D., Guerin, M., Pety, J. Abergel, A., & Roueff, E. 2004, *A&A*, 417, 135

Tulej, M., Kirkwood, D. A., Pachkov, M., & Maier, J. P. 1998, ApJ, 506, L69
Woodin, R., Foster, M. S., & Beauchamp, J. L. 1980, J. Chem. Phys., 72, 4223

Table 1. Some reactions and rate coefficients^{a,b}

R ₁	R ₂	P ₁	P ₂	α	β	γ
e-	C4H	C4H-		2.00(-9)	-0.5	
e-	C5	C5-		3.30(-8)	-0.5	
e-	C5H	C5H-		9.00(-10)	-0.5	
e-	C6	C6-		1.70(-7)	-0.5	
e-	C6H	C6H-		6.00(-8)	-0.5	
e-	C7	C7-		5.00(-7)	-0.5	
e-	C7H	C7H-		2.00(-7)	-0.5	
e-	C8	C8-		1.70(-7)	-0.5	
e-	C8H	C8H-		6.00(-8)	-0.5	
e-	C9	C9-		5.00(-7)	-0.5	
e-	C9H	C9H-		2.00(-7)	-0.5	
e-	C10	C10-		1.70(-7)	-0.5	
e-	C10H	C10H-		6.00(-8)	-0.5	
C4H-	PHOTON	C4H	e-	1.80E-09	0.0	2.0
C5-	PHOTON	C5	e-	3.00E-09	0.0	1.5
C5H-	PHOTON	C5H	e-	3.70E-09	0.0	1.5
C6-	PHOTON	C6	e-	1.30E-09	0.0	2.0
C6H-	PHOTON	C6H	e-	1.50E-09	0.0	2.0
C7-	PHOTON	C7	e-	2.40E-09	0.0	1.5
C7H-	PHOTON	C7H	e-	3.00E-09	0.0	1.5
C8-	PHOTON	C8	e-	1.10E-09	0.0	2.0
C8H-	PHOTON	C8H	e-	1.40E-09	0.0	2.0
C9-	PHOTON	C9	e-	1.60E-09	0.0	2.0
C9H-	PHOTON	C9H	e-	2.00E-09	0.0	2.0
C10-	PHOTON	C10	e-	1.00E-09	0.0	2.0
C10H-	PHOTON	C10H	e-	1.40E-09	0.0	2.0

^aRate coefficients $k = \alpha(T/300)^\beta \exp(-\gamma/T)$ in units of $\text{cm}^3 \text{s}^{-1}$

^bHerbst, in preparation.

Table 2. IRC+10216 hydrocarbon anion chemistry model results

Species	Column density (cm ⁻²)	Peak abundance rel. to H ₂	Observed column density (cm ⁻²)
C ₄ H	1.3×10^{15}	2.1×10^{-6}	$2 - 9 \times 10^{15}$ (1, 2, 3, 4)
C ₄ H ⁻	1.0×10^{13}	1.3×10^{-8}	
C ₆ H	5.7×10^{14}	1.2×10^{-6}	$0.3 - 3 \times 10^{14}$ (3, 4)
C ₆ H ⁻	1.7×10^{14}	2.6×10^{-7}	3×10^{12} (5)
C ₈ H	2.1×10^{14}	4.4×10^{-7}	5×10^{12} (4)
C ₈ H ⁻	5.8×10^{13}	1.4×10^{-7}	
C ₁₀ H	5.8×10^{13}	1.3×10^{-7}	
C ₁₀ H ⁻	2.3×10^{13}	8.3×10^{-8}	

Note. — References.— (1) Avery et al. (1992), (2) Dayal & Bieging (1993), (3) Kawaguchi et al (1995), (4) Guélin et al. (1997), (5) McCarthy et al. (2006).

Table 3. TMC-1 hydrocarbon anion chemistry model results

Species	Early time	Steady state	Observed column density (cm ⁻²)
	Column density (cm ⁻²)	Column density (cm ⁻²)	
C ₄ H	4.30×10^{13}	3.60×10^{10}	3.4×10^{14} (1)
C ₄ H ⁻	5.58×10^{10}	6.99×10^7	
C ₆ H	2.58×10^{12}	2.78×10^7	4.1×10^{12} (2)
C ₆ H ⁻	1.35×10^{11}	2.47×10^6	1.0×10^{11} (3)
C ₈ H	7.76×10^{11}	1.63×10^6	2.2×10^{11} (2)
C ₈ H ⁻	3.27×10^{10}	6.83×10^4	
C ₁₀ H	8.98×10^{10}	3.78×10^3	
C ₁₀ H ⁻	3.67×10^9	2.05×10^2	

Note. — References: (1) Guélin et al. (1982), (2) Bell et al. (1999), (3) McCarthy et al. (2006).

Table 4. TMC-1 hydrocarbon anion-to-neutral ratios C_nH^-/C_nH

n	Early time	Steady state	Observed
4	1.30×10^{-3}	1.94×10^{-3}	
6	5.23×10^{-2}	8.91×10^{-2}	2.50×10^{-2} (1)
8	4.21×10^{-2}	5.42×10^{-2}	
10	4.10×10^{-2}	5.42×10^{-2}	

Note. — References: (1) McCarthy et al. (2006).

Table 5. Horsehead Nebula hydrocarbon anion chemistry model results

Species	Peak abundance rel. to H ₂	Obs. peak abundance rel. to H ₂
C ₄ H	2.4×10^{-9}	$3.0 \pm 1.2 \times 10^{-9}$ (1)
C ₄ H ⁻	8.4×10^{-11}	
C ₆ H	9.6×10^{-12}	$1.0 \pm 0.6 \times 10^{-10}$ (1)
C ₆ H ⁻	4.5×10^{-11}	
C ₈ H	5.3×10^{-12}	
C ₈ H ⁻	9.3×10^{-11}	
C ₁₀ H	3.8×10^{-12}	
C ₁₀ H ⁻	5.5×10^{-11}	

Note. — References: (1) Teyssier et al. (2004).

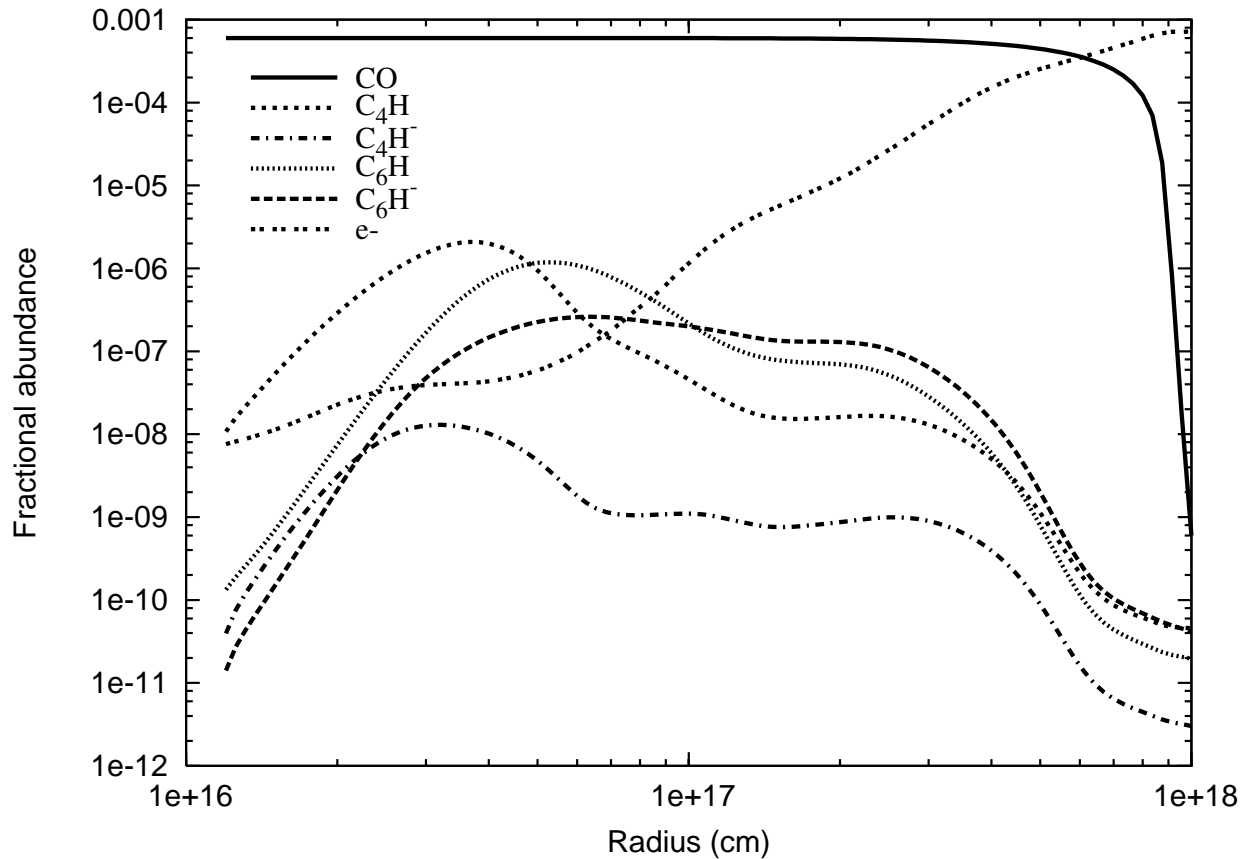


Fig. 1.— IRC+10216 circumstellar chemistry model results of hydrocarbon and anion abundances (relative to the total number density), calculated as a function of distance from the center of the star.

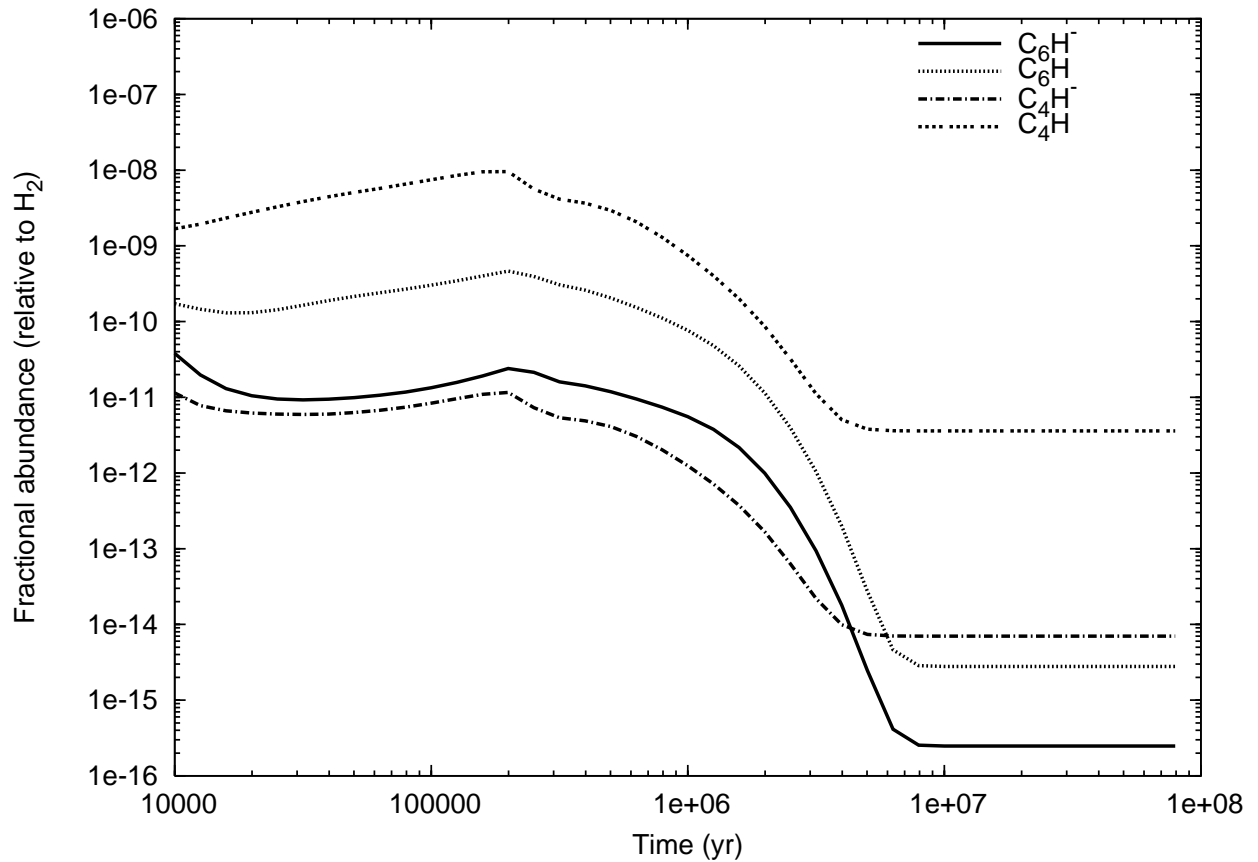


Fig. 2.— TMC-1 dark cloud chemistry model results of hydrocarbon and anion abundances (relative to H_2 density), calculated as a function of time.

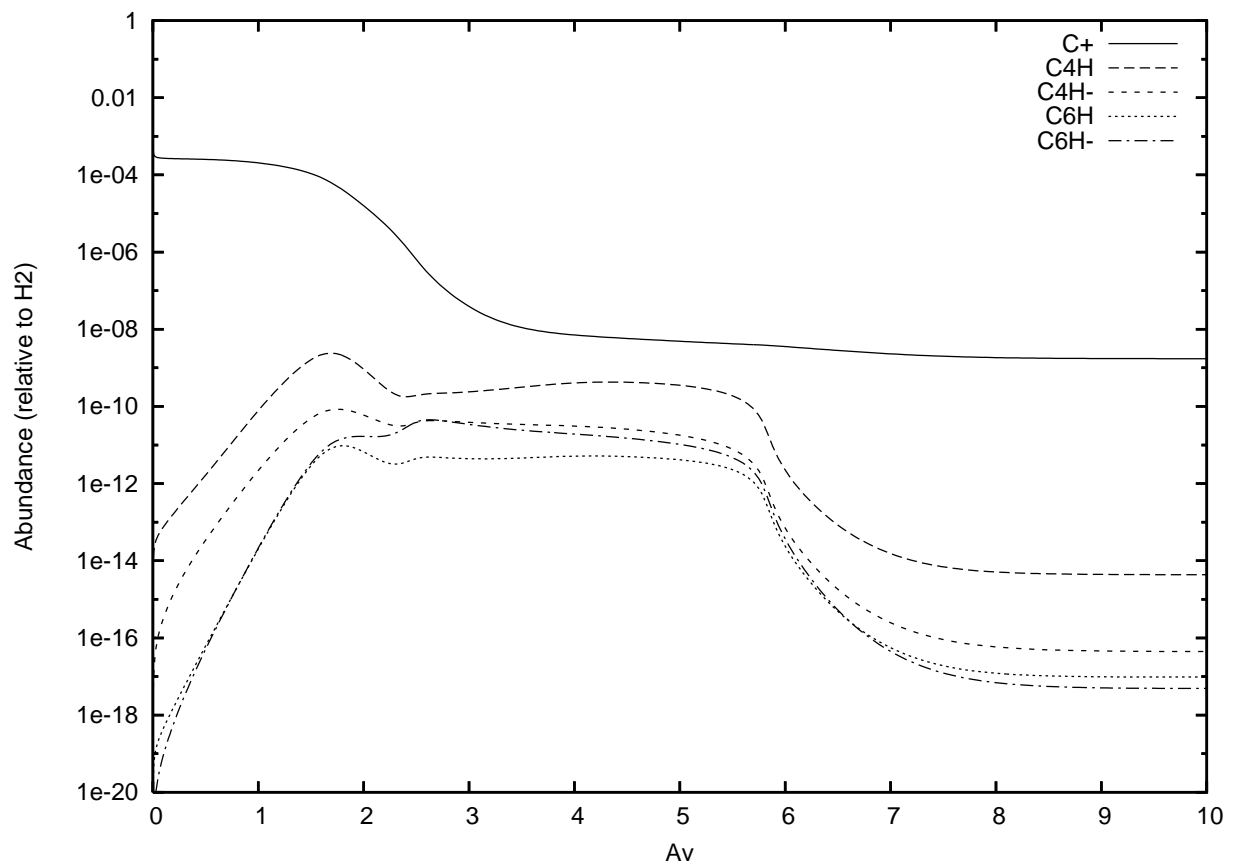


Fig. 3.— Horsehead Nebula PDR chemistry model results of hydrocarbon and anion abundances (relative to H₂), calculated as a function of A_V.